



Discovery of ((1*S*,3*R*)-1-isopropyl-3-((3*S*,4*S*)-3-methoxy-tetrahydro-2*H*-pyran-4-ylamino)cyclopentyl)(4-(5-(trifluoromethyl)pyridazin-3-yl)piperazin-1-yl)methanone, PF-4254196, a CCR2 antagonist with an improved cardiovascular profile

Robert O. Hughes^{a,*}, D. J. Rogier^a, Rajesh Devraj^a, Changsheng Zheng^b, Ganfeng Cao^b, Hao Feng^b, Michael Xia^b, Rajan Anand^b, Li Xing^a, Joseph Glenn^b, Ke Zhang^b, Maryanne Covington^b, Philip A. Morton^a, J. Matthew Hutzler^a, John W. Davis II^a, Peggy Scherle^b, Fred Baribaud^b, Anthony Bahinski^a, Zun-Li Mo^a, Robert Newton^b, Brian Metcalf^b, Chu-Biao Xue^b

^a Pfizer Global Research and Development, Chesterfield Parkway West, St. Louis, MO 63017, USA

^b Incyte Corporation, Experimental Station, Wilmington, DE 19880, USA

ARTICLE INFO

Article history:

Received 21 October 2010

Revised 10 January 2011

Accepted 11 January 2011

Available online 15 January 2011

Keywords:

CCR2 antagonist

hERG

hERG homology model

ABSTRACT

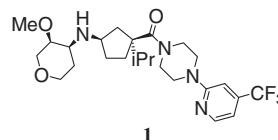
We describe the systematic optimization, focused on the improvement of CV-TI, of a series of CCR2 antagonists. This work resulted in the identification of **1** (((1*S*,3*R*)-1-isopropyl-3-((3*S*,4*S*)-3-methoxy-tetrahydro-2*H*-pyran-4-ylamino)cyclopentyl)(4-(5-(trifluoromethyl)pyridazin-3-yl)piperazin-1-yl)methanone) which possessed a low projected human dose 35–45 mg BID and a CV-TI = 3800-fold.

© 2011 Elsevier Ltd. All rights reserved.

Chemokines comprise a subset of small chemotactic cytokines classified into four groups based on cysteine residue spacing whose activities are critical for the regulation of cellular trafficking.¹ Their chemoattractive activity is mediated following binding to G-protein coupled receptors, which are well-validated drug targets. Chemokine-receptor binding initiates a cascade of intracellular signaling events mediated by receptor-associated heterotrimeric G proteins, culminating in alterations in the cytoskeleton associated with directed cell migration. Leukocyte trafficking and survival contributes importantly to chronic inflammatory states such as Rheumatoid Arthritis (RA), atherosclerosis and multiple sclerosis (MS).² The C-C class of chemokine receptors expressed on a subset of leukocytes responsible for both innate and adaptive immunity, particularly CCR1, CCR2, and CCR5, are promising and tractable targets for development of new pharmacological inhibitors of inflammation and autoimmunity.³ As these chemokine receptors are expressed on a subset of cells responsible for both innate and adaptive immunity, we and others have attempted to develop selective small molecule inhibitors of these members of the C-C chemokine receptor family. Both small molecule⁴ and biotherapeutic agents targeting CCR2 have been recently advanced into clinical trials for RA and

MS (and their modulation has been pharmacologically evaluated in both pre-clinical and clinical trials of autoimmune diseases.⁵ Herein, we report the identification of a novel and potent selective inhibitor of human CCR2 with pharmacological properties amenable to clinical evaluation.

We recently described^{6,7} **1**, Figure 1, as a potent antagonist of CCR2 as measured in binding (IC_{50} = 3.0 nM), functional chemotaxis⁸ (IC_{50} = 3.2 nM) and human whole blood (HWB, IC_{50} = 3.9 nM) assays. Compound **1** also possesses a good in vitro metabolic stability in human liver microsomes as well as an acceptable in vivo pharmacokinetic (PK) profile (rat blood clearance⁹ = 33.8 mL/min/kg and $T_{1/2}$ = 3.9 h). Taken together the potency and PK attributes of this compound predicted a relatively low human dose of 20–50 mg/BID.¹⁰ However, against hERG (1.7 μ M), an ion channel associated with cardiovascular adverse events, compound **1**



1
CCR2 IC_{50} = 3.0 nM; HWB IC_{50} = 3.9 nM
HLM Cl_{int} = 9.3 μ L/min/mg; hERG IC_{50} = 1.7 μ M

Figure 1. Chemical structure of lead compound **1**.

* Corresponding author.

E-mail address: robert.o.hughes@pfizer.com (R.O. Hughes).

showed modest affinity. Accordingly, we initiated a program directed toward improving the cardiovascular therapeutic index¹¹ (CV-TI) of **1** while maintaining excellent potency and a low human dose projection. Herein, we describe our efforts in this regard which culminated in the identification of **10**.

Reduction of a compounds overall lipophilicity, modulation of pK_a and modification of the steric environment of basic nitrogen are among the successful approaches for reducing affinity of compounds for the hERG channel which have been described.¹² Our approach to improve the cardiovascular profile of **1** was to explore modification of both the left-hand side (LHS) tetrahydropyran ring and the right-hand side (RHS) heterocycle. Based on previously established CCR2 SAR, we speculated that modifications of the RHS which were more polar than **1** and/or altered potential π -stacking interactions would be tolerated. Similarly, analysis of LHS SAR suggested modifications in this region targeted the stereo-electronic environment of the nitrogen would be fruitful. Accordingly, we designed and synthesized compounds to test these notions.

Table 1¹³ summarizes the CCR2 binding, HWB potency and hERG data collected upon replacing the trifluoro methyl pyridine

ring in **1** with five and six-membered heterocycles. Compounds **2–9** all lost CCR2 potency relative to **1**. Pyrimidine **5** was the most potent of this set possessing a CCR2 IC_{50} = 8.5 nM. Pyridazine **10** and thiazole **11** retained similar potency to **1** (8.1 nM, 8.8 nM, respectively). Isomeric thiazole **12** (28 nM) was less potent than **11**. With a CCR2 IC_{50} of 68 nM, thiadiazole was the least potent right-hand side replacement which we examined. In general, compounds **2–13** were 1.5–4-fold less potent in the CCR2 HWB assay as compared to the CCR2 binding assay. The modest shift between the CCR2 binding assay and the HWB assays is, in part, due to protein binding which is modest for this series of compounds. For instance, for compounds **1** and **10** the human fraction unbound was determined to be 29% and 79% (at 1 μ M), respectively. From the HWB perspective although all compounds were less potent than **1**, compounds **3**, **4**, **10** and **11** had sufficient potency (HWB IC_{50} s = 18.8–30.8 nM) to be attractive.

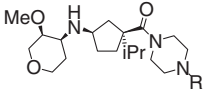
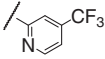
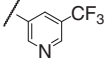
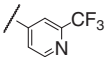
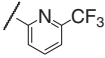
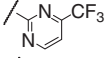
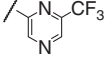
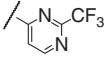
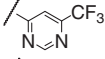
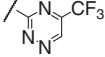
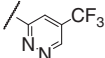
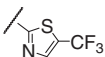
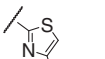
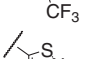
To understand the effect on RHS modifications on hERG, we determined, for some of the more potent CCR2 antagonists, the hERG IC_{50} s. Isomeric pyridines **2** and **4** had similar affinities to the hERG channel as compound **1** (hERG IC_{50} s = 2.1 and 3.9 μ M, respectively). However, as both of the isomers were less potent against CCR2 relative to **1** these compounds represented a net reduction in CV-TI. A similar combination of reduced hERG affinity and reduced CCR2 affinity for pyrazine **6**, triazine **9** and thiazole **12** resulted in a loss of CV-TI relative to compound **1** (TIs of 484-fold, 304-fold and 139-fold, respectively). An improvement in CV-TI was achieved in with compounds **3**, **7**, **8** and **10**. These compounds all possessed a significant increase in hERG IC_{50} . More importantly, CV-TIs ranged from 1400-fold for compound **7** to >4800-fold for compound **3**.

Based on the combination of binding and HWB potency as well as CV-TI the modifications represented by **3** and **10** were the most optimal of the analogs evaluated.

Examination of the properties governing the hERG affinity of the RHS modifications, revealed a relationship between measured $\log D^{14}$ and hERG IC_{50} (Fig. 2).

Following our examination of the RHS of the molecule, we turned our attention to the LHS. Table 2 shows the CCR2 binding and HWB potency as well as hERG IC_{50} data for modifications of the left-hand region of the molecule. Replacement of the methoxy group with an ethoxy group (**14** and **15**) resulted in a loss in affinity for both CCR2 and the hERG channel. As with many of the right-hand side modifications, this change in structure resulted in no improvement in overall CV-TI relative to **1** (**14**:310-fold and **15**:540-fold). Installation of an ethyl group on the THP ring to yield

Table 1
Evaluation of the right-hand aromatic region

				
Compound	R-group	CCR2 ^a	HWB ^b	hERG ^c
1		3.0	3.9	1.7
2		15.6	40.1	2.1
3		18.7	30.8	>90
4		27.5	18.8	3.9
5		8.5	18.2	4.9
6		15.8	43.7	7.6
7		25.6	71.5	35.9
8		17.8	74.7	42.6
9		29.1	45.7	8.9
10		8.1	25.7	31.3
11		8.8	18.3	ND
12		28.0	147	3900
13		68.6	ND	ND

^a CCR2 binding IC_{50} (nM).

^b CCR2 HWB IC_{50} (nM).

^c hERG IC_{50} (μ M).

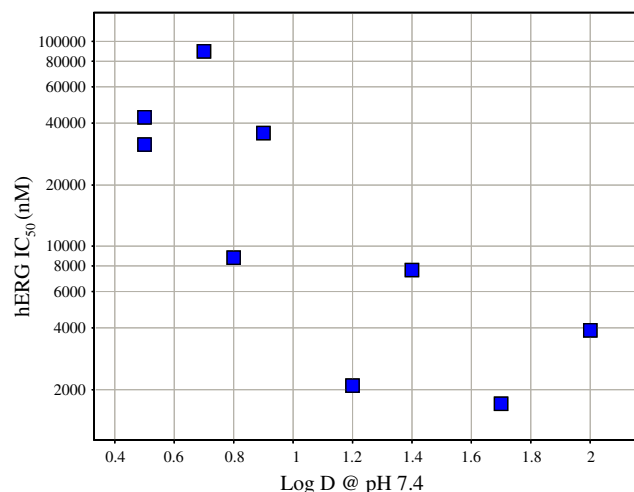
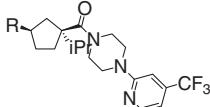


Figure 2. Correlation between $\log D$ and hERG IC_{50} for a selection of compounds listed in Table 1.

Table 2
Evaluation of the SAR of the left-hand side



Compound	R-group	CCR2 ^a	HWB ^b	hERG ^c
1		3.0	3.9	1.7
14		20.9	90.3	6.5
15		15.5	66.6	8.6
16		9.2	46.9	1.2
17		19.7	101	<0.3
18		15.4	710	0.3
19		7.3	36	1.2
20		11.2	65	1.3
21		4.5	6.4	17.0
22		9.5	23.8	1.1
23		135	23.8	1.1

^a CCR2 binding IC₅₀ (nM).

^b CCR2 HWB IC₅₀ (nM).

^c hERG IC₅₀ (μM).

16 afforded a compound with a similar profile to **1**. Replacement of methoxy group appended to the THP ring with a hydroxyl group (**18**) resulted in a five-fold loss in CCR2 potency relative to parent compound **1**. Similarly the unsubstituted pyran (**17**) resulted in a six-fold loss in CCR2 potency. Furthermore, both alterations results in a significantly increased affinity for the hERG channel. Diastereomeric bicyclic compound **19** and **20** were both slightly less potent against CCR2, but possessed an increased affinity to the hERG channel. Compound **21**, methylation of the secondary nitrogen, possessed nearly identical binding and HWB potency to **1**. Interestingly, compound **21** was 10-fold less potent against hERG than compounds **1**. However, compound **21** had poor microsomal stability (HLM Cl_{int} = 58 μL/min/mg). We suspected that the tertiary nitrogen was the likely metabolic soft spot and, accordingly, synthesized diastereomeric cyclic isomers **22**¹⁵ and **23**. Only the fast running isomer, **22**, possessed appreciable activity against CCR2 (IC₅₀ = 9.5 nM). Both compounds possessed a similar hERG IC₅₀ of 1.1 μM.

Similar to our analysis of structure–property trends governing hERG affinity on the RHS of the molecule, we undertook an analysis of the LHS. Interestingly, in this region of the molecule we found

that measures of molecular size correlated well with hERG affinity. Properties such as van der Waals volume, surface area and molecular weight correlated much better with hERG affinity than log *D*, c log *P* or tPSA. Shown in Figure 3 is the relationship between hERG and calculated van der Waals volume.

In an effort to better understand the underlying reasons for the trends in LHS and RHS SAR/SPR, we constructed a homology model of the channel.¹⁶ This model was derived from the crystal structure of the bacterial channel KcsA hybridized to a form between the closed and open states of the channel. Figure 4 shows the prototype compound **1** docked in this model. This model enable rationalization of the data which we collected. Specifically, on the RHS of the molecule in addition to a reduction of polarity a π–π interaction with PHE656 appears to be important. On the LHS, the model suggests a tight fit of **1** in the channel which may explain the negative correlation between hERG affinity and volume.

Having delineated the SAR and SPR relationships as they relate to CCR2 and hERG potency on both the left and right hand sides of the molecule we turned our attention to combining the best

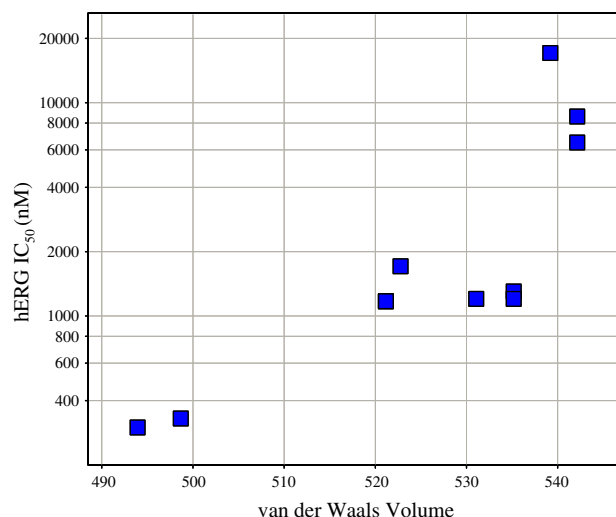


Figure 3. Correlation between van der Waals volume (Å³) and hERG IC₅₀ for the LHS modifications shown in Table 2.

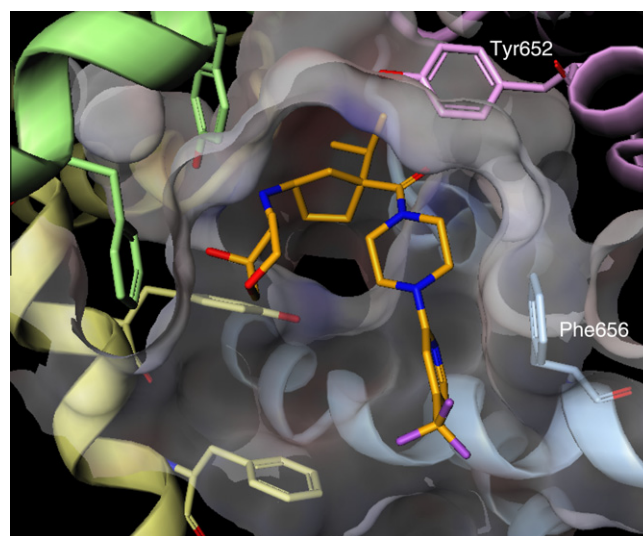
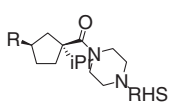


Figure 4. Homology model of the hERG channel with compound **1**. Key interactions and features of the SAR are visible. In particular, the π–π interaction between **1** and PHE656 and the tight fit of **1** on the LHS as drawn.

Table 3
Combination of the LHS and RHS


Compound	R-group	RHS ^a	CCR2 ^b	HWB ^c
24		Pyridazine ^d	31.9	73.9
25		4-Pyridine ^e	121	ND
26		Pyridazine ^d	41	ND
27		Pyridazine ^d	13	500
28		4-Pyridine ^e	49.2	ND
29		4-Pyridine ^e	55.1	ND

^a RHS = Right-hand side group.^b CCR2 binding IC₅₀ (nM).^c CCR2 HWB IC₅₀ (nM).^d 5-(Trifluoromethyl)pyridazinyl.^e 4-(Trifluoromethyl)pyridinyl.

substituents from each region of the molecule. Table 3 shows the results of this study. *N*-Methyl pyridazine analog **24** was approximately three-fold less potent in both CCR2 binding and HWB assays compared to the parent **10**. Consistent with what we observed in the pyridyl series (Table 3) this compound was also slightly less potent against hERG (IC₅₀ = 52.8 μM) as compared to **10** (IC₅₀ = 31.3 μM). Cyclic compound **25** lost significant potency against CCR2. Reflecting the increased polarity of this compound relative to **22** this was stable in human liver microsomes (Cl_{int} < 7 μL/min/mg; **22**: Cl_{int} = 17 μL/min/mg). Of the bicyclic compounds **26–29** only **27** retained good potency against CCR2 (IC₅₀ = 13 nM). This compound, however, was weakly potent in HWB (IC₅₀ = 500 nM) and poorly stable in human microsomes (Cl_{int} = 58 μL/min/mg).

As we found no improvement over compounds **3** and **10** in RHS/LHS evaluation from the perspective of potency and CV-TI, we further profiled these compounds. Table 4 summarizes additional data collected for compounds **3** and **10**. In the functional chemotaxis assay compounds **10** (IC₅₀ = 7.7 nM) was determined to be twice as potent as compound **3** (IC₅₀ = 18.4 nM). In vitro, both compounds appeared to be moderate substrates for the p-glycoprotein (PGP) efflux pump. Neither compound was turned over appreciably by human liver microsomes. In vivo¹⁷, compound **10** displayed moderate clearance and V_d while compound **3** had a significantly increased Cl and V_d. Additionally, while compound **10** did not inhibit CYP 3A4, compound **3** inhibited 3A4 31% at 3 μM possibly due to the partially exposed pyridine nitrogen. Human dose projections for the both of the compounds further underscored the overall superiority of compound **10**.

In summary, we have described the systematic optimization of the compound **1** focused, primarily, on the improvement of CV-TI. This work resulted in the identification of **10** ((1*S*,3*R*)-1-isopropyl-3-((3*S*,4*S*)-3-methoxy-tetrahydro-2*H*-pyran-4-ylamino)cyclopentyl)(4-(5-(trifluoromethyl)pyridazin-3-yl)piperazin-1-yl)methanone, PF-4254196) which possessed a low projected

Table 4
Additional data for compounds **10** and **3**

Property	3	4
log D ^a	0.7	0.5
CCR2 CTX ^b	18.4	7.7
CYP Inh ^c	31% 3A4	<3%
	4.5/6.7	3.1/6.1
MDCK ^d	<7	<7
HLM Cl _{int} ^e	78/18.4	33/5.4
Rat Cl/Vd/MRT/%F ^f	3.2/ND	2.8/50%
Dose Projection ^g	100–125 mg	35–45 mg

^a Determined at pH 7.4.^b CCR2 Chemotaxis (nM).^c CYP Inhibition measured at 3 μM (3A4, 2C9, 2D6, 1A2); for compound **3** 2C9, 2D6 and 1A2 <3%.^d Permeability in wild-type MDCK. A→B/efflux ratio.^e Human Liver Microsomal Clearance μL/min/mg of protein.^f Pharmacokinetic parameters in rat following 1mpk PO and IV doses; estimated from non-compartmental analysis. Plasma Cl = mL/min/kg; %F = Bioavailability.^g BID dose projections based on trough (C_{min}) concentration = HWB IC₈₀, and human predicted clearance and Vd using single-species scaling approaches (as in footnote 9).

human dose 35–45 mg BID and a CV-TI = 3800-fold. Further examination¹⁸ of this compound emphasized its quality and, accordingly, we nominated it for clinical development. Further details on this compound will be described in due course.

References and notes

- Baggiolini, M. *Nature* **1998**, 392, 565.
- Mackay, C. R. *Nat. Immunol.* **2008**, 9, 988; Bromley, S. K.; Mempel, T. R.; Luster, A. D. *Nat. Immunol.* **2008**, 9, 970; Charo, I. F.; Ransohoff, R. M. *N. Engl. J. Med.* **2006**, 354, 610.
- Das, A. M.; Brodmerkel, C. M. *Drug Discovery Today: Ther. Strategies* **2006**, 3, 381.
- Struthers, M.; Pasternek, A. *Curr. Top. Med. Chem.* **2010**, 10, 1278.
- Haringman, J. J.; Kraan, M. C.; Smeets, T. J.; Zwinderman, K. H.; Tak, P. P. *Ann. Rheum. Dis.* **2003**, 62, 715; Vergunst, C. E.; Gerlag, D. M.; Lopatinskaya, L.; Klareskog, L.; Smith, D.; van den Bosch, F.; Dinant, H. J.; Lee, Y.; Wyant, T.; Jacobsen, E. W.; Baeten, D.; Tak, P. P. *Arthritis Rheum.* **2008**, 58, 1931; Haringman, J. J.; Gerlag, D. M.; Smeets, T. J. M.; Baeten, D.; van den Bosch, F.; Bresnihan, B.; Breedveld, F. C.; Dinant, H. J.; Legay, F.; Gram, H.; Loetscher, P.; Schouder, R.; Woodworth, T.; Tak, P. P. *Arthritis Rheum.* **2006**, 54, 715.
- Zheng, C.; Cao, G.; Xia, M.; Feng, H.; Glenn, J.; Anand, R.; Zhang, K.; Huang, T.; Wang, A.; Kong, L.; Li, M.; Galya, L.; Hughes, R. O.; Devraj, R.; Morton, P.; Rogier, D. J.; Covington, M.; Baribaud, F.; Shin, N.; Scherle, P.; Diamond, S.; Yeleswaram, S.; Vaddi, K.; Newton, R.; Hollis, G.; Friedman, S.; Metcalf, B.; Xue, C.-B. *Bioorg. Med. Chem. Lett.* **2010**, submitted for publication.
- Compound **1** is structurally related to MK-0812; see leading Ref. 4 for more information on the Merck series of compounds.
- Sihn, N.; Baribaud, F.; Wang, K.; Yang, G.; Wynn, R.; Covington, M. B.; Feldman, P.; Gallagher, K. B.; Leffert, L. M.; Lo, Y. Y.; Wabg, A.; Xue, C.-B.; Newton, R. C.; Scherle, P. A. *Biochem. Biophys. Res. Commun.* **2009**, 387, 251.
- Blood/plasma ratio in the rat for compounds **1** was determined to be **3**.
- In the early phase of compound evaluation, human dose projection was based upon: single species allometric scaling of rat PK to give the projected human PK and maintaining, at steady state, sufficient compound levels to cover the HWB IC₈₀ at trough. For details on the scaling procedure see: Hosea, N. A.; Collard, W. T.; Cole, S.; Maurer, T. S.; Fang, R. X.; Jones, H.; Kakar, S. M.; Nakai, Y.; Smith, B. J.; Webster, R.; Beaumont, K. J. *Clin. Pharmacol.* **2009**, 49, 513.
- hERG IC₅₀/CCR2 IC₅₀ was used as first approximation of cardiovascular therapeutic index.
- Jamieson, C.; Moir, E. M.; Rankovic, Z.; Wishart, G. J. *Med. Chem.* **2006**, 17, 5029.
- Synthetic routes to the compounds described in this paper are related to those describe in Ref. 6 and Trujillo, J. I.; Huang, W.; Hughes, R. O.; Rogier, D. J.; Turner, S. R.; Devraj, R.; Morton, P.; Xue, C.-B.; Cao, G.; Covington, M. B.; Newton, R. C.; Metcalf, B. *Bioorg. Med. Chem. Lett.* **2010**, submitted for publication.
- Log Ds were measured at pH 7.4.
- All compounds described in this article are single enantiomers; generally, these compounds were purified from diastereomeric mixtures via chiral chromatography. The LHS of the molecules were installed by reductive alkylation resulting in the major isomers having the cis relationship between the amine and the beta substituent. For particularly interesting compounds, absolute stereochemical assignment was confirmed by X-ray crystallography.
- Construction of a hERG homology model involved several computational treatments in sequence. Initially a crude model was built from the crystal structure of KcsA (PDB: 1K4C) representing the closed state of the ion channel. The model was then aligned onto the open form crystal structure of MthK (PDB: 1LNQ), which was used as a guide to translate the initial model into an

intermediate form between the closed and the opened states (BMCL, 2005, 15, 1737). Affording an outward rotation of S6 helices and re-optimization of the side chain conformations, the final model represents a partially open state and was used for docking the ligands. All homology modeling and energy optimization were conducted within Maestro molecular modeling suite (Schrodinger, Inc. www.schrodinger.com). Compound **1** was docked into the hERG channel using FlexX (BioSolveIT GmbH, www.biosolveit.de/flexx/) employing CONCORD generated three-dimensional conformation. No partial charges were precomputed and the FlexX parameters were set to default. More

than a hundred docking poses were generated. Selection of the final pose was guided by docking scores as well as visual inspection of the modeled ligand–protein complex.

17. IV: 2mpk ($n = 3$) vehicle: 70% PEG400/20% 0.05 M citrate buffer/10% ethanol, pH 5; PO: 2 mpk ($n = 3$) vehicle: 0.5% methylcellulose/0.1% Tween 80 in 50 mM citric acid, pH 5; CI = mL/min/kg.
18. For instance, wide ligand panel selectivity, genetic toxicity assays as well as multi-day toxicological studies in rat and cynomolgus.